Open Access

Journal of Energy and Power Technology

LIDSEN Publishing Inc.

Original research

Improving the Engine Efficiency Using a New Combined Refrigeration Cycle for Low-Temperature Heat Source (Waste Heat Recovery)

Koorosh Goudarzi *, Mohammad Reza Zare

Yasouj University, Yasouj 75918-74831, Iran; E-Mails: kgoudarzi@yu.ac.ir; mohrezazare95@gmail.com

* **Correspondence:** Goudarzi K; E-Mail: kgoudarzi@yu.ac.ir

Academic Editor: Wahidul K. Biswas

Special Issue: Control and Optimisation of Waste- to- Energy Systems

Journal of Energy and Power Technology
2022, volume 4, issue 2
doi:10.21926/jept.2202020

Received: April 19, 2022
Accepted: May 30, 2022
Published: June 08, 2022

Abstract

Passenger and commercial internal combustion engines have relatively large dissipated thermal energy sources that can be used for initiating thermodynamic refrigeration cycles at low temperatures while improving engine efficiency. Researchers have focused on combined power-refrigeration cycles in past studies. This paper presents the operation and performance of a new combined refrigeration system driven by waste heat recovery within the internal combustion engines. For this purpose, the effects of several parameters on the performance of the cycle are examined. Results show that an increase in the engine water temperature, exhaust gas temperature, part-load ratio (PLR), generator temperature, as well as adsorption evaporator temperature had a positive effect on the performance of the cycle. However, the rise in condenser temperature of the adsorption cooling system leads to bad performance. Also, the results indicate that the application of the adsorption refrigeration cycle in the combined cooling cycle, along with the increase in the refrigeration cycle performance by up to 65%, also improves the efficiency of the internal combustion engine.

Keywords

Combined refrigeration cycle; waste heat recovery; internal combustion engine

1. Introduction

In the past few decades, many studies have been conducted on the heat energy recovery from internal combustion engines, and various power and refrigeration cycles were introduced. Meanwhile, most researchers have introduced power cycles and methods to improve their efficiency [1-13]. Some researchers also introduced refrigeration cycles powered by waste heat energy in internal combustion engines [14-16]. Power and refrigeration generation are two basic needs that can be met simultaneously with a combined power and refrigeration system. These systems form an efficient way to exploit low-cost resources. There are many ways to assist in the cogeneration of power and refrigeration. Wang et al. proposed an integrated power and refrigeration system with CO_2 fluid to recover the heat loss from an internal combustion engine [17]. Zheng et al. proposed a hybrid power and refrigeration system based on the Kalina cycle [18]. Xia et al. developed a combined power and cooling system, which comprised of an organic Rankine cycle (ORC) and an ejector refrigeration cycle for the cascade utilization of waste heat from an internal combustion engine [19]. Wang et al. investigated a model library of common components in thermodynamic systems, and dynamic simulation models of three cascade systems, including an electric-cooling cogeneration system, a double-effect absorption refrigeration system, and a double-stage organic Rankine cycle, were recognized [20]. He et al. studied the steady-state experiment, energy balance, and exergy analysis of exhaust gas to improve the recovery of the waste heat of an internal combustion engine (ICE) [21]. They considered the different characteristics of the waste heat of exhaust gas, cooling water, and lubricant, a combined thermodynamic cycle for waste heat recovery of ICE. The combined thermodynamic cycle consists of two cycles: the organic Rankine cycle (ORC), for recovering the waste heat of lubricant and high-temperature exhaust gas, and the Kalina cycle. Cao et al. proposed a novel auxiliary trigeneration system for a ship based on the engine waste heat to produce electricity, cooling, and freshwater [22]. The system consists of a regenerative organic Rankine cycle (RORC) with R600 working fluid, a lithium-bromide/water single-effect absorption chiller, and a humidification dehumidification (HDH) desalination unit. Alklaibi and Lior investigated the waste heat recovery (WHR) of a diesel engine for power generation and refrigeration [23]. They initiate waste heat recovery (WHR) from diesel engines for the generation of power by using organic Rankine cycle (ORC) systems and by providing refrigeration using absorption refrigeration systems (ARS) and adsorption cooling systems (ACS).

As mentioned above, in most previous studies, many power cycles powered by waste heat recovery of the internal combustion engine were designed and investigated to improve engine efficiency. An alternative method for improving engine efficiency is the use of refrigeration cycles that implement the waste heat energy of the engine. In recent studies, researchers have focused on combined power-refrigeration cycles to improve the efficiency of internal combustion engines. A new combined refrigeration cycle is introduced and investigated thermodynamically in this study. In this combined cooling cycle, the adsorption refrigeration cycle is used, given its important advantages along with an optimized absorption refrigeration cycle. The important idea is that the desired energy source (heat dissipation in the internal combustion engine) is a low-temperature energy source and therefore, the best thermodynamic cycle that can perform well with a low-temperature energy source is the absorption refrigeration cycle. On the other hand, by adding the

physical absorption refrigeration cycle, and by having the same features and also having no moving parts and energy, a suitable combined refrigeration cycle can be achieved.

2. System Description

Figure 1 shows the schematic of a combined refrigeration cycle that is powered by the waste heat of an internal combustion engine. The internal combustion engine shaft is used for generating power within the generator. The jacket water loop is a loop of water that passes through the engine; hence there must be another hot water loop to extract the waste heat of the jacket water, which is done by a heat exchanger (JX). As the red dashed line indicates, the exhaust gas from the engine and the hot water loop is used as heating sources in the absorption cycle. As shown in Figure 1, there is a collector/adsorber that is the connection point of the absorption cycle with the exhaust gases, which re-enters the adsorption cycle from this part.

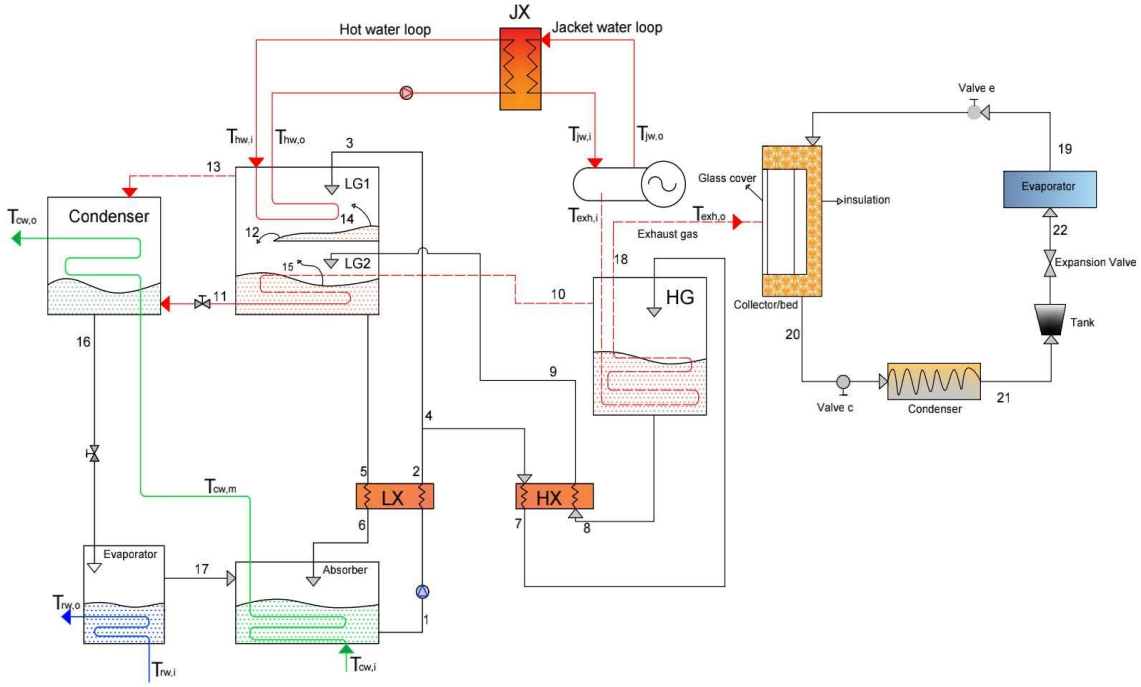

Figure 1 Schematic of a combined refrigeration cycle.

The main components of the combined cycle included the high pressure (HG) and low-pressure generators (LG), condensers, evaporators, absorbers, high temperature, low-temperature heat exchangers, collectors, adsorbers, and pressure relief valves and tanks. It should be noted that LG1 is above LG2 and LG2 is related to HG. In processes 1 to 2, the pump passes lithium bromide-water solution through the heat exchanger and receives a part of the heat from processes 3 to 4, the heating goes up, and a part of the solution goes down to the pressure generator, and the other part moves to the high-temperature heat exchanger. During 3, the resulting solution flows from 2 to the low-pressure generator. In processes 4 to 7, the solution enters the heat exchanger, the temperature rises, and finally enters the high-pressure generator. In processes 8 to 9, the solution in HG enters the heat exchanger, and some of its heat is to the opposite solution and enters LG2. In

state 10, the hot gases in HG are passed into a tube through LG2 to cool the gases into liquid, and finally, in step 11, after passing through a pressure relief valve and reducing the pressure to the condenser pressure, it enters the condenser. After performing processes 10 to 11 and passing the solution through LG2, the solution in LG2 is heated until a part of it turns into steam. The hot water ring enters LG1 and releases some of its heat, and the temperature decreases and comes out of LG1. Some heat enters LG1 through the hot water ring, causing a part of the solution in LG1 to evaporate. The vapors in LG1 and LG2 leave the generator and enter the condenser. In state 16, after passing through a pressure relief valve, the pressure of the solution of the condenser decreases and enters the evaporator. The solution enters the absorber in the next process. The liquid solution in LG2 enters the heat exchanger and releases a part of its heat to solution 2, and enters the absorber. A water pipe passes through the absorber and condenser to capture some of the gas, and a water pipe enters the evaporator to slightly heat the solution present inside the evaporator. The hot water ring enters the heat exchanger, the other side of which consists of the water jacket ring, which cools the engine. In the next step, the exhaust gas passes through the HG, from which some of the heat is given to the generator, then it leaves the generator and enters the collector. The methanol solution passes through the collector, and the output exhaust gas from HG enters the collector. The methanol solution is further heated and evaporated. In state 20, the steam enters the condenser and cools, and in state 17, the liquid methanol enters the tank. The presence of valves e and c is for the isolation of the collector. The initial temperature of the collector is equal to the outlet temperature of HG, and its pressure is approximately equal to the pressure of the evaporator. Finally, the solution enters the evaporator and heats up a bit, and these steps are repeated frequently.

3. Mathematical Models and Thermodynamic Analysis

The mathematical model of energy analysis for each component is recognized based on the principles of mass and energy conservation, and there are several major physical processes in the proposed energy equation and exergy balance equation of the combined refrigeration cycle. Each physical component in the refrigeration system can be defined through a set of mathematical equations. For the analysis of this combined cycle, assumptions that facilitate the cycle modeling process are made without significantly reducing the accuracy of the results. These assumptions are:

(1) The combined refrigeration system operates at a steady state, and pressure losses inside the pipes are ignored.
(2) Heat losses to the environment in the condenser, pumps, generator, and evaporator are neglected.
(3) The working fluid at the evaporator outlet is saturated vapor. The state of the condenser outlet is saturated liquid, and its temperature is assumed to be approximately 6 °C higher than the temperature of the environment.
(4) The flow across the throttle valve is isenthalpic.
(5) The isentropic efficiencies of pump 1 and pump 2 are assumed to be 0.85.
(6) The entire solution outlet from the generators and absorbers is in an equilibrium state.
(7) The flows occurring in the heat exchangers are regarded as counter flows.
(8) The mass flow rate of the solution, cooling water, as well as methanol are constant, and the vapor methanol behaves as a perfect gas.

(9) The specific heat of the desorbed or adsorbed methanol is considered a part of the bulk.
(10) The temperature in each of the components, i.e., the adsorber, desorber, condenser, and evaporator, remains constant throughout the whole component.

Table 1 shows the equations for the adsorption cycle. Equation (1–1) is called the Dubinin-Astakhov (D-A) equation that shows the mass of methanol adsorption in the collector [24]. Equation (2–1) shows that the amount of heat required for the adsorption or desorption of a unit of methanol is isothermal heat (ΔH). R is the methanol gas constant. During the isentropic heating phase, the collector is heated by the gauge and the value of X is maximum, and the heat is obtained from Equation (3–1) to Equation (6–1). For the isentropic desorption step, the collector moves toward the desorption and the mass of the methanol decrease to the state where X is minimized such that the heat of this process is obtained from Equation (7–1) to Equation (10–1). The temperature relations of the adsorption cycle (T_{sd}, T_{sa}) are given by Haster et al. and are calculated by Equations (11–1) and (12–1) [25]. The amount of heat that the evaporator takes from the refrigerant to cool is obtained by Equation (13–1). ΔX is the difference between the largest and the smallest amount of X, and the COP of the adsorption cooling cycle is obtained from Equations 14–1.

Table 1 Equations related to the adsorption cycle.

N	Formulas
1–1	$X(T,p) = w_0\rho_m(T)\exp\left(-\mathrm{D}\left(\mathrm{T}\ln\frac{P_s(T)}{P}\right)^n\right)$
2–1	$\Delta H = L_m(T) + RT\ln\left(\frac{P_s(T)}{P}\right) - \frac{RT}{nD}\frac{dln\rho_m}{dT}\left(Tln\frac{P_s}{P}\right)^{1-n}$
3–1	$Q_T^{1-2} = Q_w^{1-2} + Q_{AC}^{1-2} + Q_m^{1-2}$
4–1	$Q_w^{1-2} = m_W C_{pw}(T_{sd} - T_{ad})$
5–1	$Q_{AC}^{1-2} = m_{ac}C_{P_{Ac}}(T_{sd} - T_{ad})$
6–1	$Q_m^{1-2} = m_{AC}X_{max}\int_{T_{ad}}^{T_{sd}} C_{pl}dT$
7–1	$Q_T^{2-3} = Q_w^{2-3} + Q_{AC}^{2-3} + Q_m^{2-3}$
8–1	$Q_w^{2-3} + Q_{AC}^{2-3} + Q_m^{2-3}$
9–1	$Q_{AC}^{2-3} = m_{ac}C_{P_{Ac}}(T_g - T_{sd})$
10–1	$Q_m^{2-3} = m_{AC}\int_{T_{sd}}^{T_g} XC_{pl}dT$
11–1	$T_{sd} = \frac{T_{con}T_{ad}}{T_{ev}}$
12–1	$T_{sa} = \frac{T_g T_{ev}}{T_{con}}$
13–1	$Q_{ev} = m_{ac}\Delta x\left[L_m(T_{ev}) + \int_{T_{con}}^{T_{ev}} C_{pl}dT\right]$
14–1	$COP_{ad} = \frac{Q_{ev}}{Q_T^{1-2} + Q_T^{2-3}}$

The equations for the absorption cycle are shown in Table 2. Using Equation 2–1, the logarithm temperature difference can be calculated for each cycle. The efficiency of heat exchangers is

expressed as Equation (2–2). Equations (3–2) to (5–2) are equilibrium equations that can be used to obtain mass or mass fractions or unknown heat or enthalpy. For the components HG, LG1, condenser, evaporator, and absorber, heat can be calculated by using Equations (6–2). The heat energy generated by LG2 is obtained from Equations (7–2). The pump operation is obtained from Equations (8–2). The coefficient of performance (COP) for the single effect and double effect cycles can be calculated from Equations (9–2) and Equations (10–2). The cycle energy ratio is used for calculating the energy efficiency and it can be calculated by Equations (11–2). In the above equations,T_0 is 25 °C and P_0 is 1 atm. Primary energy efficiency (PEE) is defined as the ratio of output energy to primary energy consumption. External energy includes electrical output from the internal combustion engine and the output heat and cold output from the absorption cycle. This coefficient is calculated using Equations (12–2). Energy efficiency for the combined cooling cycle is indicated by the efficiency coefficient (COP):

$$COP_{combined} = \frac{Q_e + Q_{ev}}{Q_{exh} + Q_{jw} + Q_T^{1-2} + Q_T^{2-3} + W_p} \quad (3)$$

Table 2 Equations related to the absorption cycle.

N	Formulas
1–2	$\Delta T = \frac{\left(T_{flow1,i} - T_{flow2,0}\right) - \left(T_{flow1,o} - T_{flow2,i}\right)}{\log\left[\frac{\left(T_{flow1,i} - T_{flow2,0}\right)}{\left(T_{flow1,o} - T_{flow2,i}\right)}\right]}$
2–2	$\varepsilon = \frac{h_{flow1,i} - h_{flow1,o}}{h_{flow1,i} - h_{flow2.i}}$
3–2	$\sum(m_i\omega_i) - \sum(m_o\omega_o) = 0$
4–2	$Q + \sum m_i h_i - \sum m_o h_o = 0$
5–2	$\sum m_i - \sum m_0 = 0$
6–2	$Q = C_{p,flow} m_{flow} \lvert T_{flow,I} - T_{flow,o} \rvert$
7–2	$Q_{lg2} = m_8(h_9 - h_8)$
8–2	$W_p = m_{a,o}\frac{\left(P_{hg} - P_a\right)}{eta_p \rho_1}$
9–2	$COP_{hw} = \frac{m_{11'}(h_{13} - h_{12})}{Q_{jw}}$
10–2	$COP_{exh} = \frac{(m_8 + m_{11'})(h_{13} - h_{12})}{Q_{exh}}$
11–2	$eta_{exergy} = \frac{Q_e\left(\frac{T_o}{T_{rw}} - 1\right)}{Q_{jw}\left(1 - \frac{T_o}{T_{jw}}\right) + Q_{exh}\left(1 - \frac{T_o}{T_{exh}}\right) + W_p}$
12–2	$PEE = \frac{W_{el} + Q}{Q_{fuel,Ice}}$

Physical properties of methanol, characteristics of activated carbon, the baseline parameters used in the simulation cycle, thermodynamic parameters in different mixed effects in normal conditions, and the parameters of different flows of mixed effect cycle in normal conditions are shown in Tables 2-7, respectively.

Table 3 Physical properties of methanol.

Parameters	Equations
$\boldsymbol{L_m}$	$L_m = 11.28 \times 10^{-8}T^3 - 10.1045 \times 10^{-3}T^2 + 0.07092T + 643.984$
$\boldsymbol{P_s}$	$P_s = 133.33 \times \exp\left(18.5875 - \frac{3626.55}{T - 34.29}\right)$
$\boldsymbol{\rho_m}$	$\rho_m = -1.01655 \times 10^{-5}T^3 + 8.65 \times 10^{-3}T^2 - 3.3388T + 1283.315$
$\boldsymbol{C_{pl}}$	$C_{pl} = 0.9811\exp(0.0032T)$

Table 4 Characteristics of activated carbon types.

Activated carbon	Base	$\boldsymbol{\omega_0.10^3(\frac{m^3}{kg})}$	D.$\boldsymbol{10^7}$(1/K)	n	$\boldsymbol{C_{pAC}(\frac{kj}{K})}$
G32-H	coconut	0.482	0.194	2.59	0.95

Table 5 The baseline parameters used in the simulated cycle.

Symbol	Parameter	Value	Unit
$\boldsymbol{C_{pw}}$	Specific heat of the wall	0.480	kJ/kg.K
$\boldsymbol{C_{pv}}$	Specific heat of the gas	1.82	kJ/kg.K
$\boldsymbol{m_{ac}}$	Mass of the AC	21	kg
$\boldsymbol{m_w}$	Mass of the water	5	kg
R	Gas constant	259.5	J/kg.K
$\boldsymbol{C_w}$	Specific heat of the water	4.18	kJ/kg.K
$\boldsymbol{T_{ad}}$	Adsorption temperature	25	°C
$\boldsymbol{T_{con}}$	Condensation temperature	30	°C
$\boldsymbol{T_{ev}}$	Evaporation temperature	-3	°C

Table 6 Thermodynamic parameters in different of mixed effect in normal condition.

Point	Mass Flow rate (kg/s)	Enthalpy (kJ/kg)	Concentration	Pressure (kPa)	Temperature (°C)
1	0.248	99.8	0.573	0.82	38
3	0.185	171.18	0.573	6.63	73.89
5	0.233	208.17	0.609	6.63	84.85
6	0.233	132.31	0.609	0.82	44.77
7	0.062	286.52	0.573	92	129.84
8	0.058	347.31	0.612	92	155

9	0.058	224.02	0.612	6.63	92.19
10	0.004	2787.96	0	92	155
11	0.004	407.6	0	92	97.29
12	0.178	196.57	0.596	6.63	82
14	0.00716	2655.03	0	6.63	82
15	0.00344	2660.36	0	6.63	84
16	0.015	159.32	0	6.63	38
17	0.015	259.97	0	0.87	5

Table 7 Parameters of different flows of mixed effect cycle in normal conditions [25].

Flows	Inlet temperature (°C)	Outlet temperature (°C)	Mass flow rate(kg/s)
Exhaust gas	670.4	170	0.0235
Hot water	87	82	1.06
Refrigeration Water	12	7	1.64
Cooling water	30	35	3.36

4. Results and Discussion

In this study, a new combined refrigeration cycle that is powered using waste heat recovery of an internal combustion engine is introduced and analyzed by using the first and second laws of thermodynamics. Performance parameters such as COP, PEE, and exergy efficiency are analyzed with respect to the engine water temperature, exhaust gas temperature, part-load ratio (PLR), generator temperature, adsorption evaporator temperature, and adsorption condenser temperature.

Figure 2, Figure 3 and Figure 4 show the effect of the engine hot water temperature on the operation of the combined refrigeration cycle. As shown in Figure 2, as $T_{hw,i}$ grows, the COP increases. The range of changes in the COP of the combined cooling cycle is 1.14 to 1.36, which is higher than the absorption cycle, whose range of changes lies from 0.83 to 1.2.

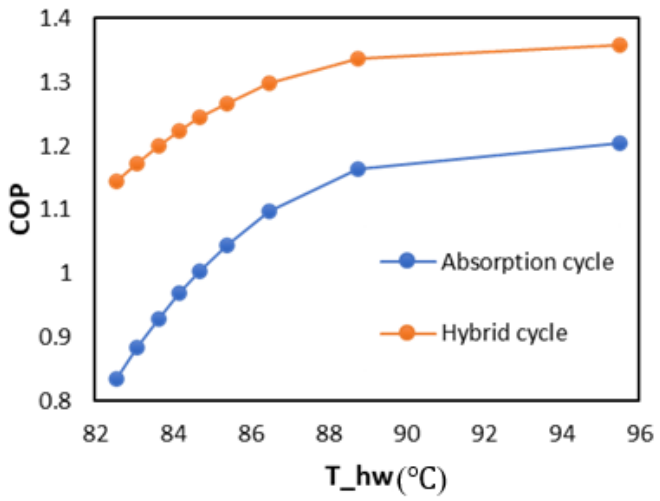

Figure 2 Influence of engine hot water temperature on COP V (T_e = 5 °C, T_c = 38 °C, T_{hg} = 155 °C, T_{ev} = -3 °C, T_{con} = 30 °C, T_{ad} = 25 °C, T_g = 110 °C).

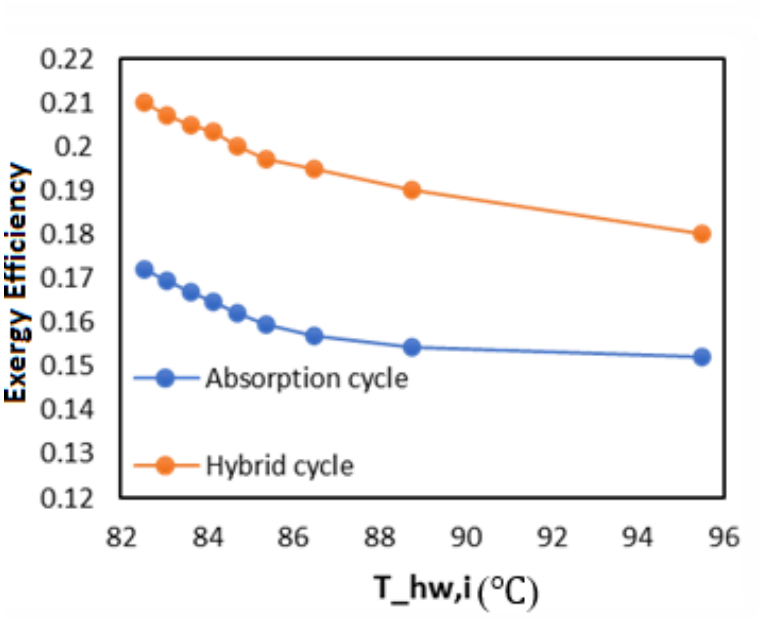

Figure 3 Influence of engine hot water temperature on COP (T_e = 5 °C, T_c = 38 °C, T_{hg} = 155 °C, T_{ev} = -3 °C, T_{con} = 30 °C, T_{ad} = 25 °C, T_g = 110 °C).

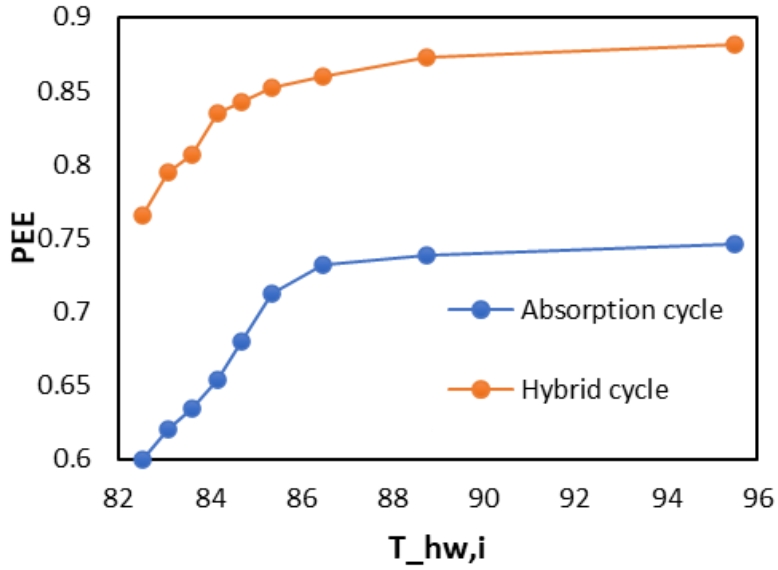

Figure 4 Influence of engine hot water temperature on exergy efficiency (T_e = 5 °C, T_c = 38 °C, T_{hg} = 155 °C, T_{ev} = -3 °C, T_{con} = 30 °C, T_{ad} = 25 °C, T_g = 110 °C).

As shown in Figure 3, as $T_{hw,i}$ rises, and the exergy efficiency decreases. The range of changes in the exergy efficiency of the combined cycle is 0.21 to 0.18, which is higher than the absorption cycle, whose range of changes lies between 0.17 to 0.15. As shown in Figure 4, as $T_{hw,i}$ grows, primary energy efficiency increases. The range of changes in the PEE of the combined cooling cycle is from 0.76 to 0.88, which is higher than the absorption cycle, whose range of changes is 0.60 to 0.74.

The effect of the exhaust gas inlet temperature on the combined cooling cycle as well as the mixed effect absorption cycle is shown in Figure 5, Figure 6 and Figure 7. As shown in Figure 5, as $T_{exh,i}$ increases the COP increases. The range of changes in the COP of the combined cooling cycle

is 0.90 to 1.20, which is higher than the absorption cycle, whose range changes from 0.85 to 0.94. As shown in Figure 6, as $T_{exh,i}$ grows, and exergy efficiency decreases. The range of changes in exergy efficiency in the combined cycle lies from 0.20 to 0.18, which is higher than the absorption cycle, whose range of changes lies from 0.17 to 0.16. As shown in Figure 6, the PEE also increases with increasing $T_{exh,i}$. The range of changes in PEE of the combined cooling cycle lies from 0.81 to 0.9, which is higher than the absorption cycle, whose range of changes lies from 0.8 to 0.87.

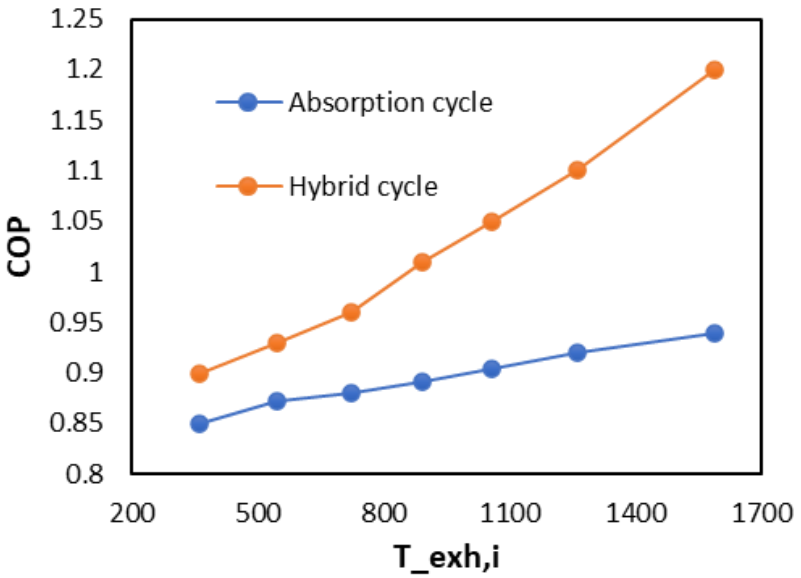

Figure 5 Influence of exhaust gas temperature on COP (T_e = 5 °C, T_c = 38 °C, T_{hg} = 155 °C, T_{ev} = -3 °C, T_{con} = 30 °C, T_{ad} = 25 °C, T_g = 110 °C).

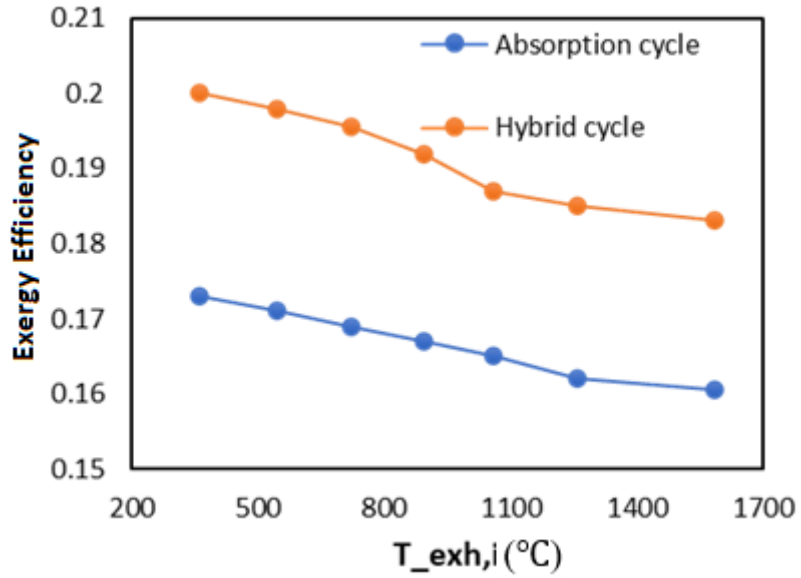

Figure 6 Influence of exhaust gas temperature on exergy efficiency (T_e = 5 °C, T_c = 38 °C, T_{hg} = 155 °C, T_{ev} = -3 °C, T_{con} = 30 °C, T_{ad} = 25 °C, T_g = 110 °C).

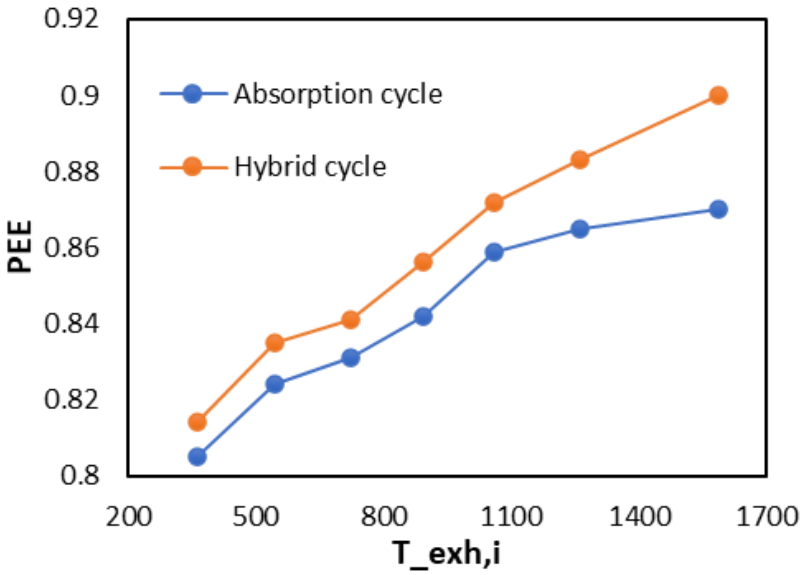

Figure 7 Influence of exhaust gas temperature on PEE (T_e = 5 °C, T_c = 38 °C, T_{hg} = 155 °C, T_{ev} = –3 °C, T_{con} = 30 °C, T_{ad} = 25 °C, T_g = 110 °C).

The PLR is the ratio of the electric output to the external electrical value of the engine. The value of this coefficient is from 0 to 1. This ratio has a significant effect on the heat dissipation of the cycle [13]. Figure 8, Figure 9 and Figure 10 show the effect of PRL on the combined cycle and the mixed effect absorption cycle. As shown in Figure 8, the COP increases with an increase in PRL. The change of COP in the combined refrigeration cycle is from 1.11 to 1.22, which is higher than the absorption cycle, whose change lies from 0.78 to 0.96. As shown in Figure 9, when the PRL increases, the exergy efficiency of the cycle decreases. The range of changes in the exergy efficiency in the combined cooling cycle is from 0.23 to 0.20, which is higher than the absorption cycle, whose range of changes is from 0.18 to 0.16. High cooling power usually occurs due to high-temperature differences, which means an excessive lack of exergy, and according to the second law of thermodynamics, the combined cooling cycle reduces heat loss to a greater extent. As shown in Figure 10, the PEE increases with the increase in PRL. The range of changes in PEE in the combined cycle lies from 0.67 to 0.82, which is higher than the absorption cycle, whose range of changes lies from 0.59 to 0.74.

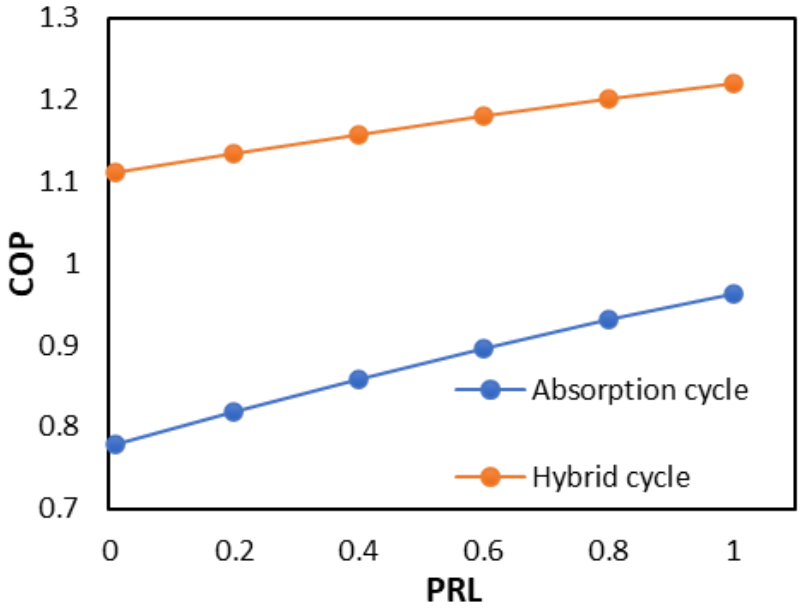

Figure 8 Influence of PRL on COP (T_e = 5 °C, T_c = 38 °C, T_{hg} = 155 °C, T_{ev} = -3 °C, T_{con} = 30 °C, T_{ad} = 25 °C, T_g = 110 °C).

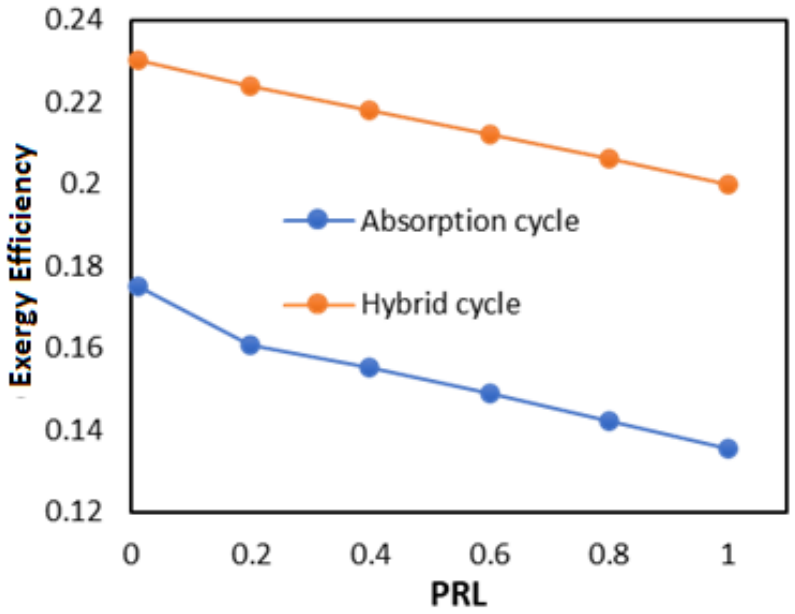

Figure 9 Influence of PRL on exergy efficiently (T_e = 5 °C, T_c = 38 °C, T_{hg} = 155 °C, T_{ev} = -3 °C, T_{con} = 30 °C, T_{ad} = 25 °C, T_g = 110 °C).

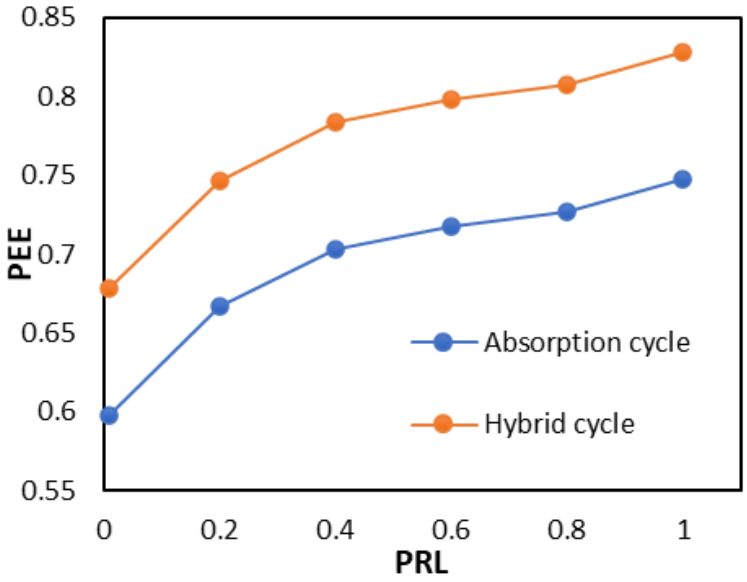

Figure 10 Influence of PRL on PEE (T_e = 5 °C, T_c = 38 °C, T_{hg} = 155 °C, T_{ev} = -3 °C, T_{con} = 30 °C, T_{ad} = 25 °C, T_g = 110 °C).

The effect of the generator temperature on the combined cooling cycle and the adsorption cycle is shown in Figure 11, Figure 12 and Figure 13. As shown in Figure 11, as T_g grows, the COP increases. The change of COP in the combined cycle is from 1.06 to 1.15, which is higher than the adsorption cycle, whose change is from 1.05 to 1.12. Also, the results presented in Figure 12 show that the efficiency of the cycle exergy decreases with increasing T_g. The efficient change of exergy in the combined cooling cycle is from 0.19 to 0.17, which is higher than the adsorption cycle, whose change lies from 0.16 to 0.14. As shown in Figure 13, as T_g grows, PEE increases. The changes of PEE in the combined cycle are from 0.62 to 0.93, which is higher than the adsorption cycle, whose range of changes is from 0.57 to 0.90.

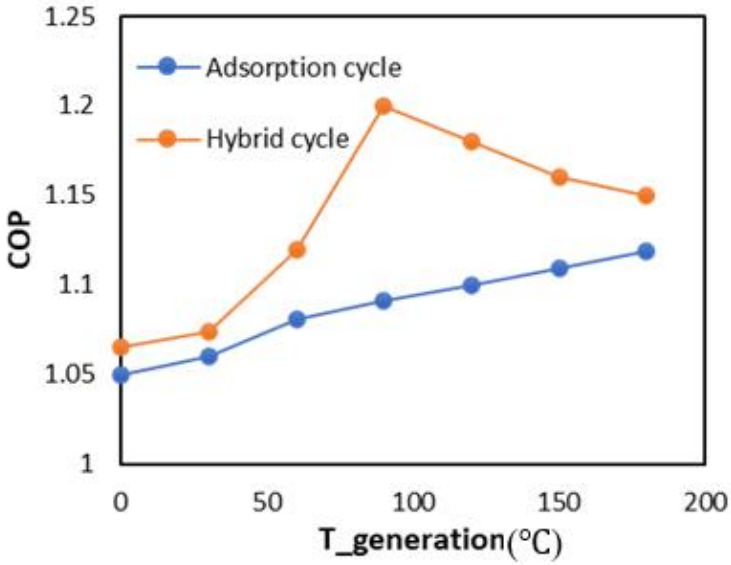

Figure 11 Influence of generator temperature on COP (T_e = 5 °C, T_c = 38 °C, T_{hg} = 155 °C, T_{ev} = -3 °C, T_{con} = 30 °C, T_{ad} = 25 °C).

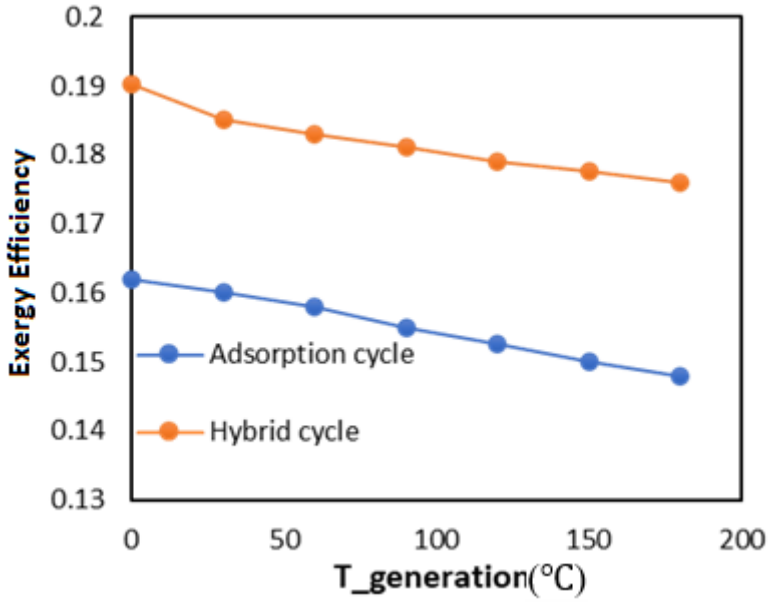

Figure 12 Influence of generator temperature on exergy efficiently (T_e = 5 °C, T_c = 38 °C, T_{hg} = 155 °C, T_{ev} = -3 °C, T_{con} = 30 °C, T_{ad} = 25 °C).

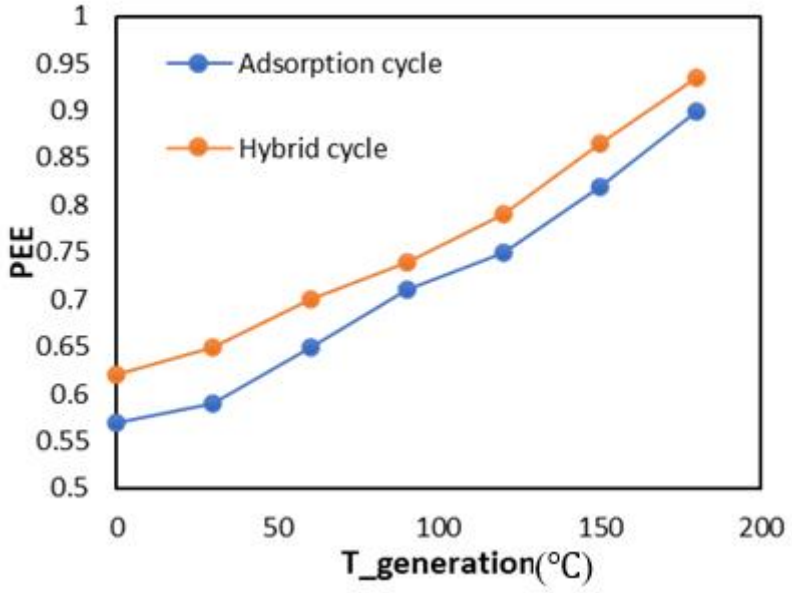

Figure 13 Influence of generation temperature on PEE (T_e = 5 °C, T_c = 38 °C, T_{hg} = 155 °C, T_{ev} = -3°C, T_{con} = 30°C, T_{ad} = 25°C).

Figure 14 and Figure 15 show the effect of the evaporator temperature of the adsorption cycle on the combined cycle and adsorption cycle. As shown in Figure 14, as T_{ev} increases, and the COP of both the cycles increases. The range of changes of the COP in the combined cycle is from 1.10 to 1.38, which is higher than the adsorption cycle, whose range of changes is from 0.64 to 0.79. Also, the results presented in Figure 15 show that the cycle exergy efficiency decreases with an increase in T_{ev}. The change in exergy efficiency of the combined cooling cycle is from 0.20 to 0.12, which is higher than the adsorption cycle, whose change is from 0.15 to 0.09. The evaporator pressure

increases as the evaporator temperature increases; this, in turn, accelerates the adsorption, increasing the mass of methanol and eventually the COP as well.

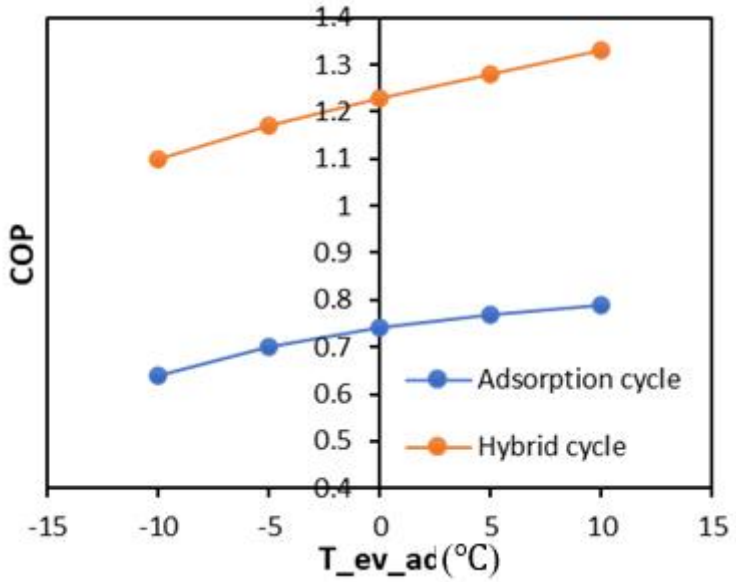

Figure 14 Influence of adsorption evaporator temperature on COP (T_e = 5 °C, T_c = 38 °C, T_{hg} = 155 °C, T_{con} = 30 °C, T_{ad} = 25 °C, T_g = 110 °C).

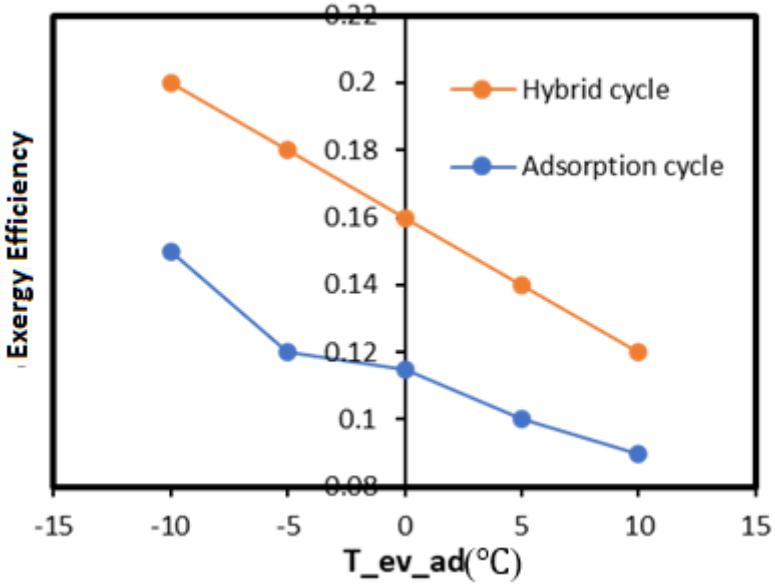

Figure 15 Influence of adsorption evaporator temperature on exergy efficiency (T_e = 5 °C, T_c = 38 °C, T_{hg} = 155 °C, T_{con} = 30 °C, T_{ad} = 25 °C, T_g = 110 °C).

The effect of the condenser temperature of the adsorption cycle on the combined cooling cycle and adsorption cycle is shown in Figure 16 and Figure 17. As shown in Figure 16, as the T_{con} increases, the COP of both the cycles decreases. The range of changes in the COP of the combined cooling cycle lies from 1.33 to 1.09, which is higher than the adsorption cycle, whose range of changes lies from 0.74 to 0.67. Also, the results presented in Figure 17 indicate that the efficiency of cycle exergy increases with an increase in T_{con}. The change of exergy efficiency in the combined

cooling cycle is from 0.13 to 0.20, which is higher than the adsorption cycle, whose change is from 0.11 to 0.15. As the condenser temperature rises, the COP decreases, which in turn increases the condenser pressure, which eventually delays the desorption phase, implying that the amount of methanol excreted decreases and the inlet heat decreases along with the condenser temperature, thereby decreasing the COP. As we can see from the results, the generator temperature has little effect on the exergy efficiency. However, the exergy efficiency is higher at low evaporator temperatures. Also, at higher condenser temperatures, the exergy efficiency indicates that the waste energy used by this system is of a higher quality.

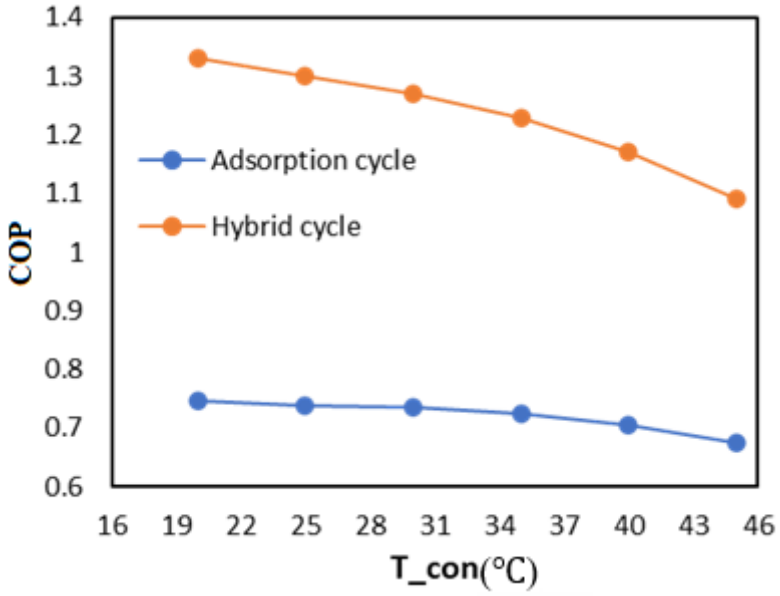

Figure 16 Influence of adsorption condenser temperature on COP (T_e = 5 °C, T_c = 38 °C, T_{hg} = 155 °C, T_{ev} = -3 °C, T_{ad} = 25 °C, T_g = 110 °C).

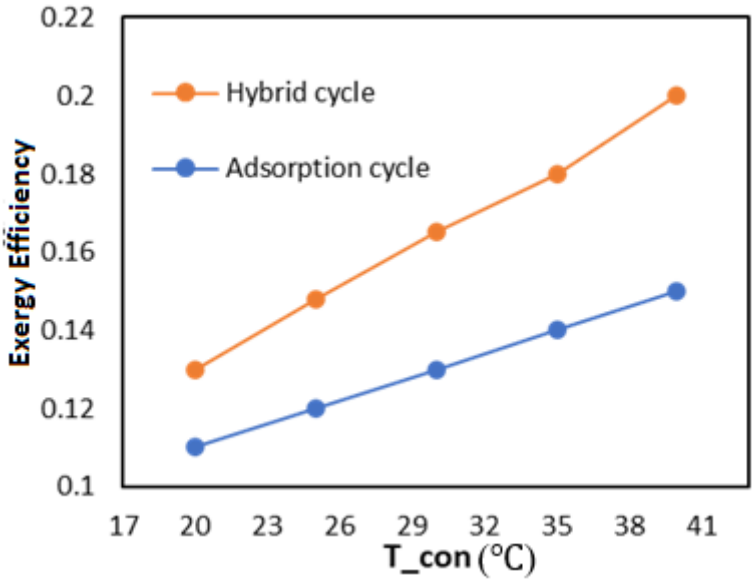

Figure 17 Influence of adsorption condenser temperature on exergy efficiently (T_e = 5 °C, T_c = 38 °C, T_{hg} = 155 °C, T_{ev} = -3 °C, T_{ad} = 25 °C, T_g = 110 °C).

5. Conclusions

In this paper, a newly combined refrigeration cycle is introduced by combining two absorption refrigeration cycles and an adsorption refrigeration cycle. The comparison of the performance of this cycle with the base cycle (absorption refrigeration cycle) was investigated by using the first and second laws of thermodynamics. The effect of important parameters such as the engine water temperature, exhaust gas temperature, PLR, as well as adsorption evaporator temperature on the energy efficiency and exergy has been investigated. The following results were obtained:

1. The exhaust gas temperature, part-load ratio (PLR), generator temperature, adsorption evaporator temperature, and the COP of the combined cooling cycle increased by up to 65% compared to the absorption refrigeration cycle when the engine water temperature was increased.
2. The COP of the combined cooling cycle decreases by increasing adsorption condenser temperature.
3. The exhaust gas temperature, part-load ratio (PLR), generator temperature, and adsorption evaporator temperature, exergy efficiency of the combined cooling cycle decrease up to 65% compared to the absorption refrigeration cycle.
4. The exergy efficiency of the combined cooling cycle increases by increasing the adsorption condenser temperature.
5. Combining the adsorption refrigeration cycle with the base cycle (absorption refrigeration) creates a good improvement in the COP of the base cycle since the COP increased up to 58%.

Nomenclature

COP	Coefficient of performance	w	mass fraction of solute
Cp	Specific heat capacity at constant pressure (kJ/kg K)	cw	cooling water
h	enthalpy (kJ/kg)	e	evaporator
HG	high-pressure generator	exh	exhaust gas
HX	high-temperature exchanger	flow	fluid in component
ICE	internal combustion engine	hg	high-pressure generator
JX	Jacket water heat exchanger	hw	hot water
LG	low-pressure generator	hx	high-temperature heat exchanger
LX	low-temperature heat exchanger	i	inlet flow
m	mass flow rate (kg/s)	jw	jacket water
P	pressure (pa)	lg	low-pressure generator
PEE	primary energy efficiently	lx	low-temperature heat exchanger
PLR	part load ratio	o	outlet flow
Q	thermal power	p	pump
R	gas constant	rw	refrigeration water
P	Pressure	ε	effectiveness of heat exchanger
T	temperature (°C)	ρ	density (Kg/m^3)
W	electric power (kW)	ac	activated carbon
Δ	difference value	v	vapor

C	specific heat (kj/kg K)	g	generator

Author Contributions

K.G. conceived of the presented idea. M.R.Z. and A.B. developed the theory and performed the computations.

Competing Interests

The authors have declared that no competing interests exist.

References

1. Yang MH, Yeh RH. Thermodynamic and economic performances optimization of an organic Rankine cycle system utilizing exhaust gas of a large marine diesel engine. Appl Energy. 2015; 149: 1-12.
2. Song J, Song Y, Gu C. Thermodynamic analysis and performance optimization of an organic Rankine cycle (ORC) waste heat recovery system for marine diesel engines. Energy. 2015; 82: 976-985.
3. Mashadi B, Kakaee A, Jafari Horestani A. Low-temperature Rankine cycle to increase waste heat recovery from the internal combustion engine cooling system. Energy Convers Manag. 2019; 182: 451-460.
4. Shi L, Shu G, Tian H, Deng S. A review of modified organic Rankine cycles (ORCs) for internal combustion engine waste heat recovery (ICE-WHR). Renew Sustain Energy Rev. 2018; 92: 95-110.
5. Di Battista D, Fatigati F, Carapellucci R, Cipollone R. Inverted Brayton cycle for waste heat recovery in reciprocating internal combustion engines. Appl Energy. 2019; 253: 113565.
6. Lu Y, Roskilly AP, Smallbone A, Yu X, Wang Y. Design and parametric study of an organic Rankine cycle using a scroll expander for engine waste heat recovery. Energy Procedia. 2017; 105: 1420-1425.
7. Zhu S, Deng K, Qu S. Energy and exergy analyses of a bottoming Rankine cycle for engine exhaust heat recovery. Energy. 2013; 58: 448-457.
8. Dubey AM. Waste heat recovery from exhaust of diesel engines using novel organic Rankine cycle configurations: A review. J Appl Eng Res. 2018; 13: 313-316.
9. Wang E, Yu Z, Zhang H, Yang F. A regenerative supercritical-subcritical dual-loop organic Rankine cycle system for energy recovery from the waste heat of internal combustion engines. Appl Energy. 2017; 190: 574-590.
10. Kim YM, Shin DG, Kim CG, Cho GB. Single-loop organic Rankine cycles for engine waste heat recovery using both low-and high-temperature heat sources. Energy. 2016; 96: 482-494.
11. Goudarzi K, Keshtgar M. Improving the engine cooling system using a power generation cycle for low-temperature heat source (heat losses in engine) instead of radiator. Appl Therm Eng. 2017; 120: 196-202.
12. Liu X, Nguyen MQ, Chu J, Lan T, He M. A novel waste heat recovery system combing steam Rankine cycle and organic Rankine cycle for marine engine. J Cleaner Prod. 2020; 265: 121502.

13. Roeinfard N, Moosavi A. Thermodynamic analysis and optimization of the organic Rankine and high-temperature Kalina cycles for recovering the waste heat of a bi-fuel engine. Fuel. 2022; 322: 124174.
14. Hamdy M, Askalany AA, Harby K, Kora N. An overview on adsorption cooling systems powered by waste heat from internal combustion engine. Renew Sustain Energy Rev. 2015; 51: 1223-1234.
15. Wang J, Wu J. Investigation of a mixed effect absorption chiller powered by jacket water and exhaust gas waste heat of internal combustion engine. Int J Refrig. 2015; 50: 193-206.
16. Wang J, Wu J, Wang H. Experimental investigation of a dual-source powered absorption chiller based on gas engine waste heat and solar thermal energy. Energy. 2015; 88: 680-689.
17. Wang S, Bai K, Xie Y, Di J, Cheng S. Analysis of combined power and refrigeration generation using the carbon dioxide thermodynamic cycle to recover the waste heat of an internal combustion engine. Math Probl Eng. 2014; 2014. DOI: 10.1155/2014/689398.
18. He M, Zhang X, Zeng K, Gao K. A combined thermodynamic cycle used for waste heat recovery of internal combustion engine. Energy. 2011; 36: 6821-6829.
19. Xia J, Wang J, Lou J, Zhao P, Dai Y. Thermo-economic analysis and optimization of a combined cooling and power (CCP) system for engine waste heat recovery. Energy Convers Manag. 2016; 128: 303-316.
20. Wang X, Shu G, Tian H, Wang R, Cai J. Dynamic performance comparison of different cascade waste heat recovery systems for internal combustion engine in combined cooling, heating and power. Appl Energy. 2020; 260: 114245.
21. He M, Zhang X, Zeng K, Gao K. A combined thermodynamic cycle used for waste heat recovery of internal combustion engine. Energy. 2011; 36: 6821-6829.
22. Cao Y, Delpisheh M, Yousefiasl S, Athari H, El-Shorbagy M, Jarad F, et al. Examination and optimization of a novel auxiliary trigeneration system for a ship through waste-to-energy from its engine. Case Stud Therm Eng. 2022; 31: 101860.
23. Alklaibi A, Lior N. Waste heat utilization from internal combustion engines for power augmentation and refrigeration. Renew Sustain Energy Rev. 2021; 152: 111629.
24. Dubinin MM, Astakhov VA. Development of the concepts of volume filling of micropores in the adsorption of gases and vapors by microporous adsorbents. Bull Acad Sci USSR Div Chem Sci. 1971; 20: 3-7.
25. Haseler LE, Robertson JM, Henry JR, Chisolm D. Absorption cycle heat pumps for domestic heating. Oxfordshire: AERE Harwell; 1978; AERE-G 104R.

Enjoy *JEPT* by:

1. Submitting a manuscript
2. Joining in volunteer reviewer bank
3. Joining Editorial Board
4. Guest editing a special issue

For more details, please visit:
http://www.lidsen.com/journal/jept